

MINIMUM X-RAY SOURCE SIZE FOR A LAMP-POST CORONA IN LIGHT-BENDING MODELS FOR AGN

M. DOVČIAK,^{1,3} AND C. DONE^{2,4}

Draft version March 2, 2024

ABSTRACT

The ‘lampost’ model is often used to describe the X-ray source geometry in AGN, where an infinitesimal point source is located on the black hole spin axis. This is especially invoked for Narrow Line Seyfert 1 (NLS1) galaxies, where an extremely broad iron line seen in episodes of low X-ray flux can both be explained by extremely strong relativistic effects as the source approaches the black hole horizon. The most extreme spectrum seen from the NLS1 1H0707-495 requires that the source is less than $1R_g$ above the event horizon in this geometry. However, the source must also be large enough to intercept sufficient seed photons from the disk to make the hard X-ray Compton continuum which produces the observed iron line/reflected spectrum. We use a fully relativistic ray tracing code to show that this implies that the source must be substantially larger than $1R_g$ in 1H0707-495 if the disk is the source of seed photons. Hence the source cannot fit as close as $1R_g$ to the horizon, so the observed spectrum and variability are not formed purely by effects of strong gravity but probably also by changes in corona and inner accretion flow geometry.

Subject headings: accretion, accretion disks — black hole physics — galaxies: active — relativistic processes — X-rays: galaxies

1. INTRODUCTION

Very broad iron $K\alpha$ lines are seen in the X-ray spectra of some Active Galactic Nuclei (AGN), indicating that the X-ray illuminated disk extends deep into the gravitational potential well of the black hole. The broadest lines, indicating the most extreme velocities and strongest gravitational fields, are seen in Narrow Line Seyfert 1 (NLS1) galaxies such as 1H0707-495 and IRAS13224-3809. Spectral fitting with a power law and its reflection over the 2-10 keV range requires that the black hole has high spin, so that the innermost stable orbit of the material in the disk is below $2R_g$, and that the line emissivity is strongly centrally peaked onto this inner disk edge, and that the spectrum is dominated by the reflected emission rather than the intrinsic continuum. These properties were first seen in MCG-6-30-15 (Wilms et al. 2001) but are much more extreme in 1H0707-495 (Fabian et al. 2009; Zoghbi et al. 2010) and IRAS13224-3809 (Ponti et al. 2010; Chiang et al. 2015). This behavior can be produced from the light-bending model (Miniutti & Fabian 2004), where a small ‘lampost’ source moves in the vicinity of the black hole changing its distance from the center. Strong relativistic effects can simultaneously boost the continuum as seen by the very inner edge of the disk, and reduce its outwards flux towards the observer when the source is very close to the event horizon of a high spin black hole. This results in a more or less constant reflection intensity, but with increasing smearing from the increasingly centrally concentrated illumination, while the observed primary power law emission drops (Miniutti & Fabian 2004).

This lamp-post geometry gives a successful framework in which to interpret the spectra and spectral variability seen in these extreme NLS1 (Fabian et al. 2009; Ponti et al. 2010; Zoghbi et al. 2010; Chiang et al. 2015). However, most mod-

eling to date has assumed a toy model of an infinitesimal (point) source. This is the simplest case for general relativistic ray tracing calculations, and Dauser et al. 2013 shows that a more physical vertically extended region can be well approximated by a point source at some effective intermediate height.

Here we try to set a lower limit on the size of an X-ray source on the spin axis from assuming that its emission is from Compton scattering of seed photons from the disk. Compton scattering conserves photon number so the corona must intercept at least as many seed photons as are required to form the observed reflected emission. We include both direct disk emission and the flux from re-processing of the illuminating source, and self consistently calculate the resulting photon density on the black hole spin axis including full general relativistic effects. We estimate this minimum radius for a spherical source, and find that it is compact but not tiny for an intrinsic $L_X/L_{\text{disk}} \sim 0.03$, as is typically observed in NLS1. This source can only fit within the space if its height above the horizon is larger than its radius (Boyer Lindquist coordinates) which limits the height to $> 10R_g$ for an on-axis source for the steepest observed spectra ($\Gamma = 3$).

However, tailoring the model to the mean spectrum of the most extreme NLS1, 1H0707-495, reveals a much stronger inconsistency. The centrally concentrated emissivity (radial index of ~ 6.6 : Fabian et al. 2012) and observed high reflected fraction ($\Omega/2\pi > 10$: Zoghbi et al. 2010) are consistent with a source at $h < 2$. However, at this low height the observed $L_{X,\text{obs}}$ is dramatically reduced from the intrinsic one, so the intrinsic source $L_X \sim 1.9L_{\text{Edd}}$. This requires a source size which is much larger than for $L_X \sim 0.03L_{\text{Edd}}$, so this cannot fit within $h < 2R_g$ for any spectral index. Some other geometry is instead required. We note that a corona which extends radially over this disk (e.g. Wilkins & Fabian 2013) will see many more photons than an on axis source.

Either the extent of the relativistic effects are overestimated from the spectra (e.g. the steepness of the radial emissivity profiles could be biased to higher values by the assumption of a constant ionization reflected spectrum (Svoboda et al. 2012) or by the effects of complex absorption (e.g. Tanaka et al.

¹ Astronomical Institute, Academy of Sciences of the Czech Republic, Boční II 1401, CZ-14100 Prague, Czech Republic

² Centre for Extragalactic Astronomy, Department of Physics, University of Durham, South Road, Durham DH1 3LE, United Kingdom

³ Michal.Dovciak@asu.cas.cz

⁴ Chris.Done@durham.ac.uk

2004; Miller & Turner 2013)), or relativistic effects alone do not control both the spectrum and variability of the source e.g. the deep dips cannot be caused by light-bending in the radially extended corona model of Wilkins et al. (2014).

2. SEED PHOTONS AND COMPTONIZATION: NON-RELATIVISTIC APPROACH

NLS1s are typically lower mass, higher mass accretion rate AGN than standard broad line Seyfert 1s. We show all calculations for mass of $10^7 M_\odot$, $L_{\text{disk}} \sim L_{\text{Edd}}$, with maximal spin, $a_* = 0.998$. We assume an inclination angle of 30° to the spin axis but this makes little difference to the results. All size scales r, h, dh (radii on the disk, height of the corona, radial size of the corona) are given in units of the gravitational radius, so $R = rR_g$, $H = hR_g$, and $dH = dhR_g$.

We first show results in a ‘Newtonian’ framework, where we assume that there is no change in photon energy or rate between the disk and the lamp-post, or between these and the observer at infinity. We also assume that light travels in straight lines, but we use the full Novikov-Thorne emissivity for ease of comparison with the fully relativistic approach in the next section. This gives the surface temperature $T(r)$ in the comoving disk frame, which peaks at T_{max} at $r = r_{\text{max}} \sim 1.6$ for $a_* = 0.998$. This inner disk temperature is high enough to produce substantial emission in the observable soft X-ray regime, especially if electron scattering within the disk acts as expected, giving a color temperature correction $f_{\text{col}} = 2.2 - 2.6$ (Ross et al. 1992; Done et al. 2012, 2013). We use $f_{\text{col}} = 2.4$ in all results shown.

The key determinant of the source size is the ratio of photons required for Comptonization compared to the photons available, which in turn is set by L_X/L_{disk} . Observations show that this is generally small in NLS1s, at around 0.02 (Vasudevan & Fabian 2007; Jin et al. 2012; Done et al. 2012). For ease of comparison to the full relativistic calculation in the next section we here include the effect of redshift from the source to the observer. For a source at height $h = 10$ then an observed $L_{X,\text{obs}} = 0.02L_{\text{Edd}}$ corresponds to a luminosity in the lamp-post frame of $L_X = 0.031L_{\text{Edd}}$. Following the light bending model, we assume that this is constant as a function of source height.

The coronal emission is soft, with power law photon index $\Gamma = 2 - 3$ (Shemmer et al. 2006; Vasudevan & Fabian 2007; Jin et al. 2012; Done et al. 2012) between a low energy cutoff set by the seed photon temperature and a high energy cutoff set by the electron temperature which we fix at 100 keV in the lamp-post frame. For a steep spectrum, the number of photons is critically dependent on the low energy cutoff, which is at $2 - 4kT_{\text{BB}}$, where T_{BB} is the temperature of the seed photons in the lamp-post frame assuming they have a blackbody distribution (e.g. Done & Kubota 2006). Hence we use the full Compton continuum shape as approximated by the NTHCOMP (Zdziarski et al. 1996; Życki et al. 1999) model in XSPEC to relate the energy flux in the spectrum to photon number for a given seed photon temperature.

The photon rate required to make the Comptonized spectrum depends also on the optical depth τ of the corona, as only a factor $(1 - e^{-\tau})$ of the photons are scattered into the tail. This depends on geometry as well as spectral index and electron temperature, and requires a fully relativistic treatment (rather than analytic approximations) for electron temperatures which are a substantial fraction of the electron rest mass as assumed here. Hence we use the XSPEC model `compps` (Poutanen & Svensson 1996) which includes all these factors.

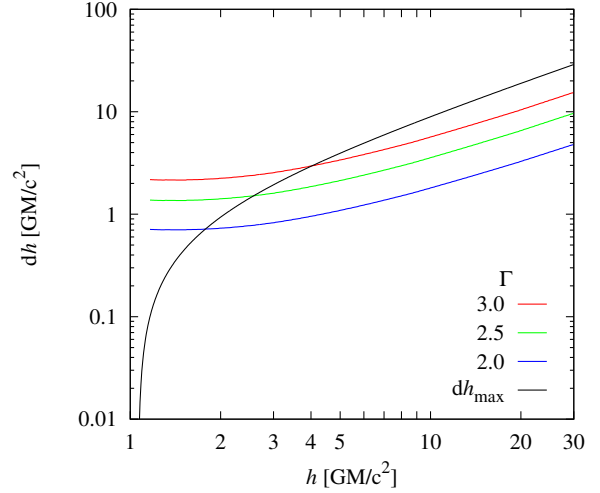


Figure 1. Newtonian radius of corona. A size scale for the corona in Newtonian approximation required to produce $L_X/L_{\text{disk}} = 0.02$ as observed at infinity for a typical NLS1 ($10^7 M_\odot$, $L_{\text{disk}} = L_{\text{Edd}}$) for $\Gamma = 2, 2.5,$ and 3 (bottom to top; corresponding to $\tau = 0.85, 0.4,$ and 0.2 , respectively) assuming $a = 0.998$. More seed photons are required for softer spectra as the source only scatters a fraction $1 - e^{-\tau}$. The photon rate intercepted by a source on axis increases for decreasing h down to $h \sim r_{\text{max}} = 1.6$, so the required source size decreases with h and then flattens for $h < r_{\text{max}}$ where the intensity is constant for isotropic emission. The black line shows the maximum radius where the source fits above the horizon.

We choose a spherical geometry with isotropic seed photons (geom=-4), where spectral indices of $\Gamma = 2, 2.5,$ and 3 correspond to $\tau = 0.85, 0.4,$ and 0.2 for $kT_e = 100$ keV. We use $T_{\text{BB}} = 0.2$ keV (Jin et al. 2013), but the derived values for τ do not depend much on this parameter. Hence the required seed photon rate, N_{seed} , needs to be larger than the rate of photons in the Compton spectrum, N_0 , by the factor $(1 - e^{-\tau})^{-1}$, so $N_0 = N_{\text{seed}}(1 - e^{-\tau})$.

These X-ray photons illuminate the disk, so can be either reflected or reprocessed (thermalized) in the disk. The fraction which thermalize, η_{th} can add to the seed photon flux from the intrinsic disk emission. Photons from the lamp-post emitted into a solid angle $d\Omega_L$ illuminate a surface area perpendicular to the light rays at the disk of $dS_{d\perp}$ at radius R (see geometry in Dovčiak et al. 2014). This corresponds to a surface area on the disk $dS_d = 2\pi R^2 dR$ where $dS_{d\perp}/dS_d = H/D$ and $D^2 = R^2 + H^2$. Then the illuminating flux on the disk is $F_{\text{ill}}(R) = L_X/(4\pi D^2) \times dS_{d\perp}/dS_d = L_X/(4\pi)H/D^3$. This leads to a rise in temperature such that $T_{\text{tot}}^4(R) = F_{\text{ill}}(R)/\sigma_{\text{SB}} + T^4(R)$. However, this increase is negligible where the ratio L_X/L_{disk} is small.

This is a somewhat surprising result in the context of the X-ray spectrum, where the lamp-post model generates an extremely centrally concentrated emissivity. However, even in a fully relativistic treatment, this concentrated illumination is small compared to the much more luminous disk emission.

The source at the height H on the disk axis with a cross-section $dS_L = \pi(dH)^2$ receives photons from the disk area dS_d into the solid angle $d\Omega_L = (d\Omega_L/dS_d) dS_d = H/D^3 2\pi R dR$. Thus the fraction of photons from the disk which illuminate the source, $dS_L \times d\Omega_L$, increases with decreasing R down to $R = H/\sqrt{2}$ where it reaches a maximum and then decreases with the further decrease of R . The rate at which photons are emitted from the disk at radius R depends on the temperature, $dN_{\text{disk}}(R) \sim T^3(R)$, and the to-

tal rate of the intercepted photons by the source is $dN_{\text{seed}} = dN_{\text{disk}}(R) \times dS_L \times d\Omega_L$ assuming that the source emits isotropically. The total seed photon rate $N_{\text{seed}} = \int_R dN_{\text{seed}}$, giving the radius of the corona, dH , from the constraint that N_{seed} needs to be such that it can make the Comptonized emission.

The seed photons have a range in temperature as they are produced over a range of radii. However, this multi-temperature seed photon distribution has a clear peak at energy E_0 , and can be fairly well approximated by a single blackbody at a temperature $T_{\text{BB}} = E_0/2.82$. This seed photon temperature is always somewhat smaller than the peak disk temperature, T_{max} , by an amount that depends slightly on the source height. For $h \lesssim r_{\text{max}}$ this reaches a maximum of $\sim 0.75T_{\text{max}}$, while for $h \gg r_{\text{max}}$ it asymptotes to $0.25T_{\text{max}}$.

The black, green and blue lines in Figure 1 show the derived source size as a function of height for $\Gamma = 2, 2.5$ and 3 for a black hole mass of $10^7 M_\odot$, $a = 0.998$, $f_{\text{col}} = 2.4$ with $L_{\text{disk}} = L_{\text{Edd}}$. The seed photon density on axis increases with decreasing h until $h \sim r_{\text{max}} \sim 1.6$ for our assumed $a = 0.998$, so the source size decreases up to this point, then tends to a constant value of a few R_g as the flux no longer rises due to the inner hole to the disk. We repeated the calculation for $10^6 M_\odot$, and for a color temperature correction of both 1 as well as 2.4, but these parameters make a negligible difference to the results. Our results are also fairly insensitive to our assumption that $L_{\text{disk}} = L_{\text{Edd}}$, as it is L_X/L_{disk} which is important. With this set to 0.031 then Γ is the main determinant of source size. Steeper spectra require more photons to make the same luminosity, and also intercept a smaller fraction of the available seed photons due to their lower optical depth. Both factors increase the seed photons required by around a factor three $\Gamma = 3$ compared to $\Gamma = 2$, so the source size is a factor $\sqrt{3 \times 3} = 3 \times$ larger for $\Gamma = 3$ than $\Gamma = 2$. Thus the source size changes from $\sim 1 - 3R_g$ as Γ increases from 2 – 3. The source is compact, as seems reasonable in view of the fast variability and micro-lensing constraints, but not tiny, as also seems reasonable in view of the energy emitted from the region.

3. FULLY RELATIVISTIC APPROACH

There are clearly a number of relativistic factors which affect this calculation. We illustrate the effect of each of these in turn in Figure 2, where the dotted black line shows the $\Gamma = 2$ results from Figure 1. Firstly the energy of the seed photons from each annulus in the disk as seen in the lamp-post frame is $kgT(r)$ where $g = E_L/E_d$ is the energy shift between the comoving disk frame and the lamp-post. For $h > r_{\text{max}}$ then this is a redshift, while for $h < r_{\text{max}}$ it is a blueshift. The photon rate received at the lamp-post depends on g^3 , so the required source size increases for $h > r_{\text{max}}$, and decreases for $h < r_{\text{max}}$ (red line: Figure 2). Note, that r_{max} in relativistic case is shifted to higher values, since the maximum temperature as perceived by the corona is $\max[g(r)T(r)]$ instead of just $T_{\text{max}} = \max[T(r)]$.

Another factor is that the curvature of space-time means that a source of given proper size extends over a smaller radial coordinate distance as the source approaches the black hole. The radial coordinate distance is important as this sets the position of the horizon, r_H , so that $dh < h - r_H$ (Boyer Lindquist coordinates). This effect means that the source radius in Boyer-Lindquist coordinates is always smaller than from the non-relativistic approach (blue line: Figure 2).

The green line in Figure 2 shows the effect of light bend-

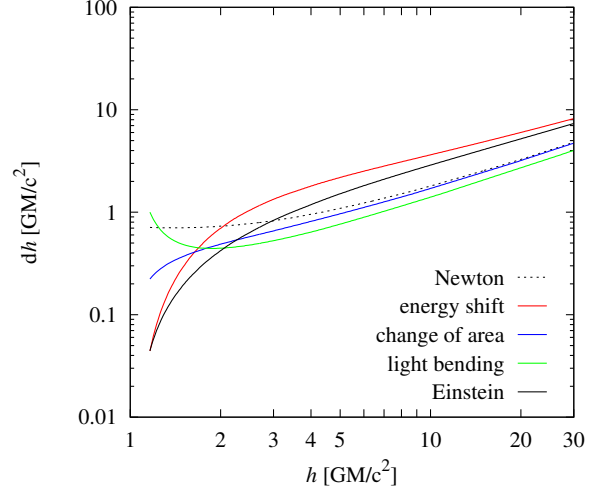


Figure 2. Contributing relativistic effects. A comparison of the size of each relativistic effect with the Newtonian results in Figure 1 for $\Gamma = 2$ (black dotted line). The major effect is from the energy shift, g , between the comoving disk and lamp-post frame as the photon rate is proportional to g^3 (red line). The change between coordinate distance and proper distance is also a factor (blue line), and these two effects are larger than light bending with aberration (green line). The black solid line shows the results including all the relativistic effects.

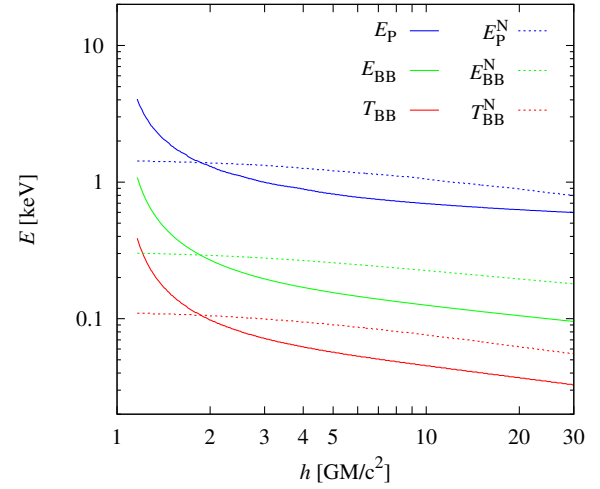


Figure 3. Photon temperature and average energy. The seed photon temperature, T_{BB} (red), average seed photon energy, E_{BB} (green), and average Comptonized photon energy, E_p (blue) evaluated in the lamp-post frame at different heights. The ‘Newtonian’ values are also shown (dotted lines).

ing and aberration on the solid angles. We use the code of Dovčiak et al. 2014 to follow the full photon geodesics, and transform the angles discussed above. However, this is not such an important effect. The solid black line in Figure 2 including all relativistic effects is dominated by the boosting/deboosting of the thermal emission.

Figure 3 shows resulting fully relativistic mean energy of seed photons and Comptonized photons in the lamp-post frame. The red solid line shows the seed photon temperature $T_{\text{BB}} = E_0/2.82$, where E_0 is the peak energy of the multicolor black body received at the lamp-post. The green solid line shows the mean seed photon energy, $E_{\text{BB}} = \int EN_{\text{seed}}(E)dE / \int N_{\text{seed}}(E)dE$ from this multicolor blackbody. The fact that it is close to $2.82T_{\text{BB}}$ shows that a single

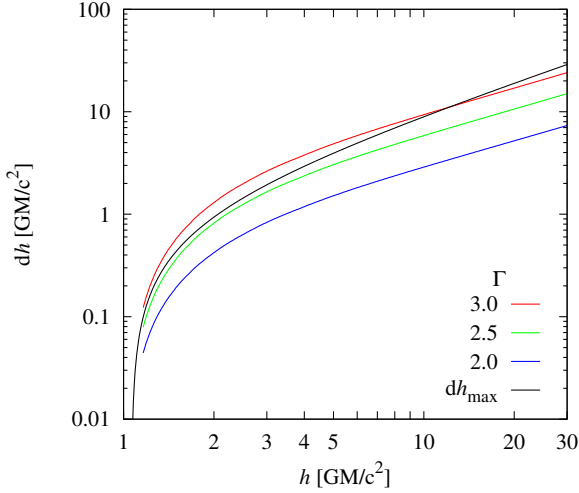


Figure 4. Corona radius in full general relativity. As for Figure 1, but accounting properly for all general relativistic effects. The radius of the source is in Boyer-Lindquist coordinates so the maximum radius for a source at height h which can fit above the horizon at r_H is $h - r_H$, (black line). A steep spectrum ($\Gamma = 3.0$: red) on the spin axis does not intercept enough flux from the disk to produce the observed Comptonized emission for $h < 12$.

blackbody is a good approximation to the shape of the seed photon distribution. The blue solid line shows the mean energy of photons in the Comptonized spectrum for the fiducial model with $\Gamma = 2$ shown in Figure 2. The dotted lines in Figure 3 show the corresponding Newtonian energies. The change in energy is much larger in the fully relativistic treatment due to the boosting/de-boosting of photons between the co-moving disk frame and the lamp-post. Thus its impact on the number of photons required in the Compton spectrum is larger than in the 'Newtonian' case. However, the power extracted from the electrons $L_e = L_X - N_0 E_{BB} = (E_p - E_{BB})N_0$ so it does not depend much on height as E_p is set by E_{BB} , and both change together for a given spectral index (see Figure 3), so this is canceled out by the opposite change in N_0 . Thus our model is consistent with the constant dissipation in the intrinsic X-ray source which is assumed in the lamp-post geometry. It comes out that about 80%, 55%, and 40% of the intrinsic primary X-ray luminosity needs to be extracted from electrons for $\Gamma = 2.0, 2.5,$ and $3.0,$ respectively.

Figure 4 shows the resulting minimum radial size estimate of the corona in full general relativity, again for $\Gamma = 2, 2.5,$ and $3.$ As before, softer spectra ($\Gamma = 2$: blue; 2.5 : green; 3 red) require a larger source size. The black line shows the maximum size, set by the constraint that the corona does not extend below the horizon. A source with $\Gamma = 2$ and 2.5 can have $dh \lesssim h - r_H$ at any height for an intrinsic luminosity of $L_X = 0.031 L_{\text{disk}}$. However, there are not enough photons on the spin axis of the black hole to make the softest spectra observed in NLS1 for a source of this luminosity at a height $< 12 R_g$.

4. APPLICATION TO 1H0707-495

1H0707-495 is one of the most extreme NLS1 in terms of the inferred relativistic effects (Fabian et al. 2009; Zoghbi et al. 2010, hereafter Z10). The 0.3-10 keV power law flux in these data from 2008 changes from $\sim 2 \times 10^{-13}$ to 2×10^{-11} erg cm 2 s $^{-1}$ (Z10), and the lowest flux episode is similar to the spectrum seen in 2011 where the inferred line

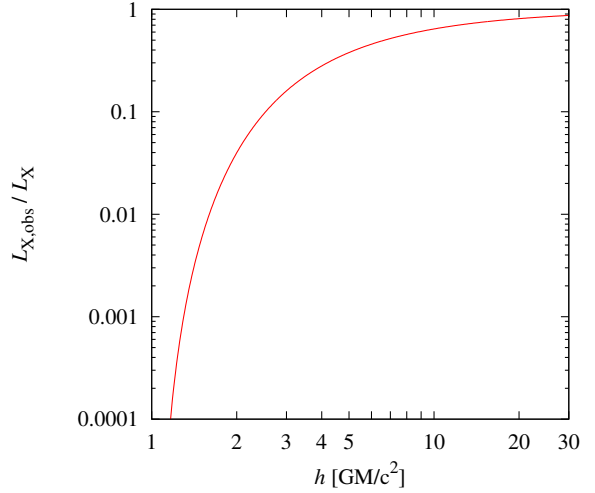


Figure 5. Flux decrease. The suppression of the intrinsic power law flux received at infinity as a function of height.

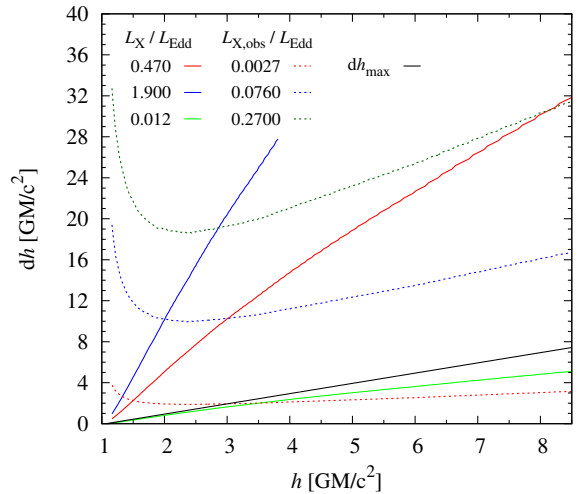


Figure 6. Size of the corona for 1H0707-495. *Solid curves* show the required radius of the spherical patch of corona for a given intrinsic luminosity. In pure light-bending scenario with constant intrinsic luminosity the patch of corona would have to change its size along these graphs as it changes its position on the axis. *Dotted curves* show the corona radius for a given observed luminosity if the primary source is located at certain height. Corona receives less thermal disk photons if it is farther away from the disk thus the radius increases with larger heights. However, for very small heights large intrinsic luminosities are needed for the same observed luminosity (see Figure 5) and thus the required radius increases rapidly.

emissivity has index of 8.8, requiring a source at $h < 1.5$ (Fabian et al. 2012, hereafter F12; see also Dauser et al. 2012; Dovčiak et al. 2014).

Hence we use $h = 1.5$ as the baseline for the lowest flux observation in 2008. The power law flux at each frequency is suppressed by the factor $g_L^2 d\Omega_L / d\Omega_{\text{obs}}$ where $g_L = E_{\text{obs}} / E_L = \sqrt{1 - 2h / (h^2 + a^2)}$, and $d\Omega_L / d\Omega_{\text{obs}}$ is the light-bending term. At such a low height, $g_L = 0.275$ (corresponding to redshift $z = 2.632$), while $d\Omega_L / d\Omega_{\text{obs}} = 0.076$. Figure 3 shows that the seed photon temperature $T_{BB} \sim 0.15$ keV in the lamp-post frame, so we redshift a Compton spectrum with $\Gamma = 3$ and this seed photon temperature to find the bolometric correction from the observed 0.3-10 keV band-pass is a factor of 2.32, so $F_{X,\text{obs}} = 4.64 \times 10^{-13}$ erg cm 2 s $^{-1}$,

or $L_{X,obs} = 0.0027L_{Edd}$. Since this is suppressed by the factor $g_L^2 d\Omega_L/d\Omega_{obs} \sim 0.0057$, the intrinsic source flux in the lamp-post frame is $F_X = 8.14 \times 10^{-11} \text{ erg cm}^2 \text{ s}^{-1}$, corresponding to $L_X = 0.47L_{Edd}$. This is substantially larger than the flux assumed in Section 3, so all radii in Figure 4 will be increased by a factor $\sim \sqrt{0.47/0.031} \sim 4$. These source sizes cannot fit within $h = 10$, let alone $h = 1.5$ for any $\Gamma = 2 - 3$.

We show the resulting source radius on a linear scale as the red solid line in Figure 6. It is always larger than the maximum source size which can fit above the horizon (black solid line). By contrast, the red dotted line shows the source size which gives the observed $L_{X,obs} = 0.0027$. The minimum source height which is consistent with the source fitting above the horizon is $h = 3$. However, at this height, relativistic effects are not so extreme and the emissivity radial power-law index is $\lesssim 4$ (Dauser et al. 2013).

The maximum X-ray flux from the source is a factor $100 \times$ larger, implying $L_{X,obs} = 0.27L_{Edd}$ (including the bolometric correction). This flux change can be produced by moving the source up to $h = 8.2$ (see Figure 5), but the dark green dotted line in Figure 6 shows that a source of this observed luminosity cannot fit anywhere on the spin axis for $h < 9$.

However, the lowest luminosity power law has large uncertainties (e.g. Z10, F12). Instead, we recalculate our results from the mean spectrum from 2008, where the power law detection is much more robust with a 0.3-10 keV flux of $6.2 \times 10^{-12} \text{ erg cm}^2 \text{ s}^{-1}$ (F12). This has an emissivity index of 6.6, which still requires a very small lamp-post height of $h < 1.5 - 2$ (Dauser et al. 2013; Dovčiak et al. 2014). We use the largest source height of $h = 2$, but this is probably an overestimate as seen by the large reflected fraction of the data. Z10 quote a ratio of reflected to power law flux of 1.3 in their 0.3-10 keV bandpass, but this requires a solid angle of $\sim 10 - 20$ for their low ionization parameter. The predicted solid angle for a lamp-post source at $h = 2$ is ~ 7 (Dauser et al. 2014).

Thus the observed reflection dominance and centrally concentrated emissivity are consistent with the lamp-post at $h \sim 2$. This gives $g_L = 0.446$ ($z = 1.240$), and a bolometric correction of 2.15, hence a flux as seen at infinity of $F_{X,obs} = 1.33 \times 10^{-11} \text{ erg cm}^2 \text{ s}^{-1}$, corresponding to $L_{X,obs} = 0.076L_{Edd}$. This is suppressed by a factor 0.04 (Figure 5), so the intrinsic luminosity in the lamp-post frame is $L_X = 1.9L_{Edd}$. This implies an even larger source size than before, with $dh \sim 10$ as shown by the blue solid line in Figure 6. Even the observed $L_{X,obs} = 0.076$ is too large a luminosity to be produced by a source on the spin axis for any $h \leq 9$ (blue dotted line).

The large intrinsic X-ray luminosities required in order to produce the observed reflected emission dramatically exceed those observed due to the strong suppression of the X-ray flux from the combined effects of redshift and light bending. Such large intrinsic luminosities require a correspondingly large source size in order to intercept sufficient seed photons. This size is inconsistent with the size scale required for the source to fit above the horizon.

The largest intrinsic luminosity which is consistent with the minimum source size which can fit above the horizon at small h is shown by the solid green line in Figure 6, which has $L_X = 0.012L_{Edd}$. This is a factor of 10 smaller than the *observed* 0.3-10 keV flux at maximum, so this cannot possibly be a viable solution. The corona would have to change its size with

height by much larger amount to increase the intrinsic primary flux to reach these observed values and then it will no longer fit above the horizon (the green solid line in Figure 6 would have to curve up to join the dark-green dotted line).

5. DISCUSSION AND CONCLUSIONS

There is no viable 'lamp-post' source geometry (small source on the black hole spin axis) which can explain the observations of 1H0707-495. The mismatch is most marked by considering the mean spectrum from 2008 (Z10; F12), where the intrinsic power law is clearly seen along with highly relativistically smeared reflection. A source which is at small enough height to explain the observed highly centrally peaked emissivity and reflection dominance has $h \lesssim 2$. However, the power law suppression from both light bending and redshift here is extreme, and requires that the observed rather small X-ray luminosity must instead represent a much larger intrinsic X-ray luminosity, of $1.9L_{Edd}$! This requires a minimum source size of ~ 10 assuming that the power law is formed by Compton up-scattering of seed photons from the disk, so it cannot have an effective mean height of $h = 2$, so it cannot reproduce the implied large reflected fraction, nor the extremely centrally peaked emissivity.

A small source at $h = 2$ could be recovered if there is an additional source of seed photons, perhaps from a strong magnetic field. A magnetic field is surely required in order to produce the lamp-post source in the first place, so it is worth exploring this possibility. To have the magnetic energy density be of the order of the X-ray energy density for $L_x \sim 2L_{Edd}$ requires $B \sim 10^6 \text{ G}$, but self-absorption will strongly limit the number of cyclo-synchrotron seed photons which can be produced (di Matteo et al. 1997).

Nonetheless, the source could easily power both the large X-ray luminosity and sustain a large magnetic field as the optical/UV emission from the outer disk in 1H0707-495 implies that the source is accreting at $\sim 200L_{Edd}$ for a maximally rotating black hole with mass of $2 \times 10^6 M_\odot$ (Done & Jin 2015). Thus it is energetically possible that the very weak observed X-rays are due to a very high intrinsic X-ray flux which is dissipated so close to the black hole that it is strongly suppressed. However, $L_X > L_{Edd}$ is a completely new requirement for NLS1. Generically these are observed to be X-ray weak even in sources where the spectra are not dominated by reflection, and the observed reflection is not strongly smeared (e.g. Jin et al. 2012).

A tiny lamp-post corona geometry cannot explain all the aspects of the X-ray data: the source must be somewhat extended. This highlights an issue with our calculations as our model simply scales the seed photon density on the spin axis to set the source size, without explicitly re-calculating the seed photon density for the off-axis extent of the source and for the expected rotation of such a source. This is clearly required, and means that the source will intercept more seed photons from the disk as the black hole spin axis minimizes the photon density. Thus a full 3D computation is required to estimate the actual size and shape of the corona. Calculations of extended source geometries have been done by e.g. Wilkins & Fabian 2012; Wilkins et al. 2014; Dauser et al. 2013, 2014. However, it seems highly unlikely that the reflecting disk can remain thin and flat for such a super Eddington flow, so the reflector geometry as well as the coronal size and shape should also be considered.

ACKNOWLEDGMENTS

The research leading to these results has received funding from the European Union Seventh Framework Programme

(FP7/2007-2013) under grant agreement n°312789. CD acknowledges STFC grant ST/L00075X/1 and thanks the FP7 strong gravity consortium for funding a visit to Prague where much of the work was done.

APPENDIX

MULTI-COLOR BLACK BODY RECEIVED BY THE CORONA

The disk emits with standard Novikov-Thorne emissivity, so forms a blackbody with temperature $T(r)$ from each radius r . We allow for the possibility of a color temperature correction, which increases the temperature by a factor f_{col} , and decreases the normalization by f_{col}^4 so as to give the same total luminosity.

Photons from the disk are emitted from a Boyer-Lindquist area $dS_{\text{d}} = 2\pi r dr$ at energy E_{d} in the local frame comoving with the disk. These are received at the lamp-post with energy E_{L} (such that $g = E_{\text{L}}/E_{\text{d}}$) from a solid angle $d\Omega_{\text{L}}$. The multi-color black body radiation received at the lamp-post from the accretion disk is $F_{\text{in}} \equiv dN/(dt dS_{\text{L}})$, i.e. the photon number density flux received at the lamp-post with a perpendicular cross-section dS_{L} . Both dS_{L} and $d\Omega_{\text{L}}$ are measured locally in the reference frame of the lamp-post. The incoming thermal photon flux has to be integrated over the disk,

$$\begin{aligned} F_{\text{in}} &= 2\pi \int_0^\infty dE \int_{r_{\text{in}}}^{r_{\text{out}}} dr r \frac{2}{f_{\text{col}}^4 h^3 c^2} \frac{E^2}{e^{E/kgT} - 1} \frac{d\Omega_{\text{L}}}{dS_{\text{d}}} \\ &= 2\pi \frac{4\zeta(3)k^3}{f_{\text{col}}^4 h^3 c^2} \int_{r_{\text{in}}}^{r_{\text{out}}} dr r \frac{d\Omega_{\text{L}}}{dS_{\text{d}}} (gT)^3, \end{aligned} \quad (\text{A1})$$

$$T = T_{\text{norm}} r^{-3/4} \left[\frac{\mathcal{L}(r)}{\mathcal{C}(r)} \right]^{1/4} \left(\frac{\dot{M}}{M_{\odot} y^{-1}} \right)^{1/4} \left(\frac{M}{M_{\odot}} \right)^{-1/2}, \quad (\text{A2})$$

$$T_{\text{norm}} \equiv f_{\text{col}} c^{3/2} \left(\frac{3}{8\pi G^2 M_{\odot} y \sigma} \right)^{1/4}, \quad (\text{A3})$$

where all symbols have their usual meanings, $\zeta(3) \approx 1.202056903159594$ is an Apéry's constant, and where $T(r)$, $\mathcal{L}(r)$, $\mathcal{C}(r)$ are given in e.g. Novikov & Thorne (1973) or Page & Thorne (1974).

DISK TEMPERATURE INCREASE DUE TO ILLUMINATION

The accretion disk is illuminated with the energy flux

$$F_{\text{inc}}(r) = g_{\text{L}} g \frac{d\Omega_{\text{L}} L_{\text{X}}}{dS_{\text{d}} 4\pi} \quad (\text{B1})$$

where we used the local area on the disc to be $dS = dS_{\text{d}}/(g_{\text{L}} g)$ (see e.g. eq. (2.8) in Dovčiak 2004) with $g_{\text{L}} = E_{\text{obs}}/E_{\text{L}}$ and $g_{\text{L}} g = E_{\text{obs}}/E_{\text{d}}$. Thus temperature will rise due to the illumination to

$$T = \left(T_{\text{BB}}^4 + \frac{\eta_{\text{th}} F_{\text{inc}}}{\sigma} \right)^{1/4} \quad (\text{B2})$$

with the η_{th} being the fraction of the illumination flux that is thermalized. For NLS1, the ratio of power in X-rays versus the intrinsic disk emission is small, so re-processing makes only a negligible effect on the photon flux.

NOTE ON THE DERIVATION OF CROSS SECTION IN BOYER-LINDQUIST COORDINATES

We define the cross section in the Boyer-Lindquist coordinates as

$$dS_{\text{BL}} = n^{\beta} d^2 S_{t\beta}, \quad (\text{C1})$$

where the unit vector $n^{\beta} = (0, p^i)/\sqrt{p^i p_i} = -(0, p^i)/(p_{\mu} U_{\text{L}}^{\mu})$ has the direction of the 3-vector of the photon momentum. We will use the fact that the cross section is the same for all observers (see e.g. eq. (2.6) in Dovčiak 2004)⁵

$$(p^{\beta} d^2 S_{\beta\alpha} - p_{\alpha} dS^{\perp}) U^{\alpha} = 0 \quad (\text{C2})$$

⁵ Here we would like to emphasize that while this equation holds true for any 4-velocity, U^{α} , i.e. for all time-like vectors, it is not valid for all space-like vectors. Indeed, if we use e.g. a vector X^{α} that lies in the area defined by $d^2 S_{\alpha\beta}$ so that the first term in the equation is zero, the second term will

be non-zero if the scalar product $p_{\alpha} X^{\alpha}$ is non-zero. Thus the 4-vector in the parenthesis of the eq. (C2) is not zero as is claimed in the eq. (2.7) in Dovčiak (2004).

for the time-like 4-vector $U^\alpha = (1, 0, 0, 0)$. In our case the locally observed U^α area is perpendicular to the photon 3-momentum, $dS_L = dS^\perp$, and further $p_t = -1$. Thus we get

$$dS_{BL} = -\frac{p^\beta d^2 S_{t\beta}}{p_\mu U_L^\mu} = g_L dS_L. \quad (C3)$$

In our calculations we use the radius, dh , of the Boyer-Lindquist proper cross-section from assuming the circular shape, $dS_{BL} = \pi dh^2$. The radius defined in this way does not equal to the change in Boyer-Lindquist coordinates. In fact the proper area that would be parallel or perpendicular with the axis would depend on the change of the BL coordinates, dh , as $\pi dh^2 \sqrt{h^2 + a^2}/h$ or $\pi dh^2 \sqrt{(h^2 + a^2)(h^2 - 2h + a^2)}/h^2$, respectively. This would lead to 9% smaller radii in the first case and 59% larger radii in the second case for the spin $a = 0.998$ and height $h = 1.5$. Thus our estimation of corona radius from proper area will not differ too much from the radius that would be given in the Boyer-Lindquist coordinates.

THE INTRINSIC X-RAY FLUX EMITTED BY THE CORONA

We assume the local X-ray emission of the corona to be given by the non-thermal Comptonization model, NTHCOMP (Zdziarski et al. 1996; Życki et al. 1999), available in the spectral fitting package XSPEC (Arnaud 1996). We compute the NTHCOMP normalization, N_L , from the observed photon flux

$$\begin{aligned} F_{X,obs}(0.3 - 10\text{keV}) &= \frac{1}{4\pi D^2} L_{X,obs}(0.3 - 10\text{keV}) = \frac{g_L^2}{4\pi D^2} \frac{d\Omega_L}{d\Omega_{obs}} L_X(0.3/g_L - 10/g_L \text{keV}) = \\ &= \frac{g_L^2}{4\pi D^2} \frac{d\Omega_L}{d\Omega_{obs}} N_L \int_{0.3/g_L}^{10/g_L} E \text{nthcomp}(E) dE. \end{aligned} \quad (D1)$$

Here we needed to use the computation of NTHCOMP luminosity in the corona frame since it depends on the temperature of the incident black-body radiation. Then the total observed luminosity, $L_{X,obs}$, and the total intrinsic photon production rate in the corona, F_{out} , are

$$L_{X,obs} = 4\pi D^2 \frac{\int_0^\infty E \text{nthcomp}(E) dE}{\int_{0.3/g_L}^{10/g_L} E \text{nthcomp}(E) dE} F_{X,obs}(0.3 - 10\text{keV}) \quad (D2)$$

and

$$F_{out} = 4\pi D^2 \left(g_L^2 \frac{d\Omega_L}{d\Omega_{obs}} \right)^{-1} \frac{\int_0^\infty \text{nthcomp}(E) dE}{\int_{0.3/g_L}^{10/g_L} E \text{nthcomp}(E) dE} F_{X,obs}(0.3 - 10\text{keV}), \quad (D3)$$

respectively.

To complete basic equations leading to our corona size estimates we conclude with the number of scattered photons that make up the intrinsic photon production rate,

$$(1 - e^{-\tau}) F_{in} dS_L = F_{out}. \quad (D4)$$

REFERENCES

- Arnaud, K.A. 1996, *Astronomical Data Analysis Software and Systems V*, eds. Jacoby G. and Barnes J., p17, ASP Conf. Series volume 101
- Chiang, C.-Y., Walton, D. J., Fabian, A. C., Wilkins, D. R., & Gallo, L. C. 2015, *MNRAS*, 446, 759
- Dauser, T., Svoboda, J., Schartel, N., et al. 2012, *MNRAS*, 422, 1914
- Dauser, T., García, J., Wilms, J., et al. 2013, *MNRAS*, 430, 1694
- Dauser, T., García, J., Parker, M. L., Fabian, A. C., & Wilms, J. 2014, *MNRAS*, 444, L100
- di Matteo, T., Celotti, A., & Fabian, A. C. 1997, *MNRAS*, 291, 805
- Done, C., & Kubota, A. 2006, *MNRAS*, 371, 1216
- Done, C., Davis, S. W., Jin, C., Blaes, O., & Ward, M. 2012, *MNRAS*, 420, 1848
- Done, C., Jin, C., Middleton, M., & Ward, M. 2013, *MNRAS*, 434, 1955
- Done, C., & Jin, C. 2015, *MNRAS*, submitted, arXiv:1506.04547
- Dovčiak, M. 2004, *Radiation of Accretion Discs in Strong Gravity*, PhD Thesis (Charles University, Prague), arXiv:astro-ph/0411605
- Dovčiak, M., Svoboda, J., Goosmann, R. W., et al. 2014, in *Proceedings of RAGtime 14-16: Workshops on black holes and neutron stars* (Silesian University in Opava), arXiv:1412.8627, in press
- Fabian, A. C., Zoghbi, A., Ross, R. R., et al. 2009, *Nature*, 459, 540
- Fabian, A. C., Zoghbi, A., Wilkins, D., et al. 2012, *MNRAS*, 419, 116 (F12)
- Jin, C., Ward, M., Done, C., & Gelbord, J. 2012, *MNRAS*, 420, 1825
- Jin, C., Done, C., Middleton, M., & Ward, M. 2013, *MNRAS*, 436, 3173
- Miller, L., & Turner, T. J. 2013, *ApJL*, 773, L5
- Miniutti, G., & Fabian, A. C. 2004, *MNRAS*, 349, 1435
- Novikov, I. D., & Thorne, K. S. 1973, in *Black holes*, ed. C. de Witt and B. S. de Witt (New York, NY: Gordon & Breach), 343
- Page, D. N., & Thorne, K. S. 1974, *ApJ*, 191, 499
- Ponti, G., Gallo, L. C., Fabian, A. C., et al. 2010, *MNRAS*, 406, 2591
- Poutanen, J., & Svensson, R. 1996, *ApJ*, 470, 249
- Ross, R. R., Fabian, A. C., & Mineshige, S. 1992, *MNRAS*, 258, 189
- Shemmer, O., Brandt, W. N., Netzer, H., Maiolino, R., & Kaspi, S. 2006, *ApJL*, 646, L29

- Svoboda, J., Dovčiak, M., Goosmann, R. W., et al. 2012, *A&A*, 545, 10
Tanaka, Y., Boller, T., Gallo, L., Keil, R., & Ueda, Y., 2004, *PASJ*, 56, L9-L13
Vasudevan, R. V., & Fabian, A. C. 2007, *MNRAS*, 381, 1235
Wilkins, D. R., & Fabian, A. C. 2012, *MNRAS*, 424, 1284
Wilkins, D. R., & Fabian, A. C. 2013, *MNRAS*, 430, 247
Wilkins, D. R., Kara, E., Fabian, A. C., & Gallo, L. C. 2014, *MNRAS*, 443, 2746
Wilms, J., Reynolds, C. S., Begelman, M. C., et al. 2001, *MNRAS*, 328, L27
Zdziarski, A. A., Johnson, W. N., & Magdziarz, P. 1996, *MNRAS*, 283, 193
Zoghbi, A., Fabian, A. C., Uttley, P., et al. 2010, *MNRAS*, 401, 2419 (Z10)
Życki, P. T., Done, C., & Smith, D. A. 1999, *MNRAS*, 305, 231